Translational Oncology 15 (2022) 101244

Contents lists available at ScienceDirect

Translational Oncology

journal homepage: www.elsevier.com/locate/tranon

Original Research

FLT3 inhibition by olverembatinib (HQP1351) downregulates MCL-1 and synergizes with BCL-2 inhibitor lisaftoclax (APG-2575) in preclinical models of *FLT3-ITD* mutant acute myeloid leukemia

Douglas D. Fang [a,1], Hengrui Zhu [a,1], Qiuqiong Tang [a], Guangfeng Wang [a], Ping Min [a], Qixin Wang [a], Na Li [a], Dajun Yang [a,b], Yifan Zhai [a,*]

[a] Ascentage Pharma (Suzhou) Co, Ltd, 218 Xinghu Street, Suzhou, Jiangsu Province, China
[b] State Key Laboratory of Oncology in South China, Collaborative Innovation Center for Cancer Medicine, Sun Yat-sen University Cancer Center, Guangzhou, China

ARTICLE INFO

Keywords:
FLT3-ITD
BCL-2
HQP1351
APG-2575
Acute myeloid leukemia

ABSTRACT

Introduction: *FLT3-ITD* mutations occur in approximately 25% of patients with acute myeloid leukemia (AML) and are associated with poor prognosis. Despite initial efficacy, short duration of response and high relapse rates limit clinical use of selective FLT3 inhibitors. Combination approaches with other targeted therapies may achieve better clinical outcomes.

Materials and methods: Anti-leukemic activity of multikinase inhibitor olverembatinib (HQP1351), alone or in combination with BCL-2 inhibitor lisaftoclax (APG-2575), was evaluated in *FLT3-ITD* mutant AML cell lines *in vitro* and *in vivo*. A patient-derived *FLT3-ITD* mutant AML xenograft model was also used to assess the anti-leukemic activity of this combination.

Results: HQP1351 potently induced apoptosis and inhibited FLT3 signaling in *FLT3-ITD* mutant AML cell lines MV-4-11 and MOLM-13. HQP1351 monotherapy also significantly suppressed growth of *FLT3-ITD* mutant AML xenograft tumors and prolonged survival of tumor-bearing mice. HQP1351 and APG-2575 synergistically induced apoptosis in *FLT3-ITD* mutant AML cells and suppressed growth of MV-4–11 xenograft tumors. Combination therapy improved survival of tumor bearing-mice in a systemic MOLM-13 model and showed synergistic anti-leukemic effects in a patient-derived *FLT3-ITD* mutant AML xenograft model. Mechanistically, HQP1351 downregulated expression of myeloid-cell leukemia 1 (MCL-1) by suppressing FLT3-STAT5 (signal transducer and activator of transcription 5) signaling and thus enhanced APG-2575-induced apoptosis in *FLT3-ITD* mutant AML cells.

Conclusions: FLT3 inhibition by HQP1351 downregulates MCL-1 and synergizes with BCL-2 inhibitor APG-2575 to potentiate cellular apoptosis in *FLT3-ITD* mutant AML. Our findings provide a scientific rationale for further clinical investigation of HQP1351 combined with APG-2575 in patients with *FLT3-ITD* mutant AML.

Introduction

Acute myeloid leukemia (AML) accounts for approximately 80% of adult acute leukemias [1]. Despite advances of clinical treatments, including eight (mainly "targeted") therapies approved by the US Food and Drug Administration (FDA) in the past 2 years, the survival of patients with AML remain suboptimal, with a 5-year survival rate of 67% in individuals younger than 20 and 25% in older persons [2].

Fms-like tyrosine kinase 3 *(FLT3)* is the most frequently mutated gene in patients with AML [3], with approximately 25% internal tandem duplication (ITD) mutations in the juxtamembrane domain and about 7% of point mutations in the tyrosine kinase domain (TKD) [4,5]. Both types of mutations constitutively activate FLT3 kinase independent of extracellular ligand stimulation and lead to activation of downstream signaling pathways, including phosphoinositide 3-kinase (PI3K), mitogen-activated protein kinases (MAPK) and signal transducer and activator of transcription 5 (STAT5). The molecular cascades result in increased cellular proliferation and decreased apoptosis in cancer cells

* Corresponding author.
E-mail address: yzhai@ascentage.com (Y. Zhai).
[1] Both the authors contributed equally to this work.

https://doi.org/10.1016/j.tranon.2021.101244
Received 10 July 2021; Received in revised form 23 September 2021; Accepted 11 October 2021
1936-5233/© 2021 Published by Elsevier Inc. This is an open access article under the CC BY-NC-ND license (http://creativecommons.org/licenses/by-nc-nd/4.0/).

[6–8]. The *FLT3-ITD* mutation is associated with a lower rate of complete remission (CR), as well as a higher death rate, and an increased risk of relapse, hence conferring a poor prognosis in AML [9–13].

As a well-validated therapeutic target in AML, multiple FLT3 inhibitors that block the constitutive kinase activity of FLT3 have been developed and shown a substantial clinical benefit in patients with FLT3 mutant AML [13,14]. Midostaurin, the first marketed FLT3 inhibitor, effectively increases the overall survival of patients with *FLT3-ITD* or D835/F697 mutated AML, and midostaurin plus chemotherapy has become the standard of care in frontline AML treatment [15]. Next generation FLT3 inhibitors, including gilteritinib (ASP2215), quizartinib (AC220) and crenolanib (CP-868,596), are more selective FLT3 inhibitors. These agents have shown promising single agent anti-leukemic activity in clinical trials, and gilteritinib and quizartinib were approved for treatment of relapsed/refractory FLT3 mutated AML [16]. However, despite the initial responses to FLT3 inhibitors in patients with AML, follow-up clinical data have shown that the efficacy of FLT3 inhibitors is limited by short duration of response and nearly inevitable relapse in most patients [17–20]. Therefore, combination approaches with a second targeted therapy may therefore be required to improve clinical outcomes.

Anti-apoptotic protein B-cell lymphoma 2 (BCL-2) is frequently dysregulated in AML. Overexpression of BCL-2 is associated with therapeutic resistance and is a biomarker for worse responses to chemotherapy in patients with AML [21–23]. In an unbiased, large-scale clustered regularly interspaced short palindromic repeats (CRISPR) screening, knockout of BCL-2 enhanced the anti-leukemic effects of FLT3 inhibitors in AML [24]. Venetoclax, a potent and selective BCL-2 inhibitor, has been developed and approved by the FDA in combination with low-dose cytarabine (LDAC) or hypomethylating agents for treatment of elderly patients with AML or those who are ineligible for intensive chemotherapy [25,26]. Inhibition of BCL-2 by venetoclax synergistically enhances the anti-leukemic activity of FLT3 inhibitors in preclinical models of *FLT3-ITD* mutant AML [27,28]. These preclinical findings indicate that co-inhibition of BCL-2 and FLT3 represents a promising therapeutic strategy for AML. The combination of venetoclax and FLT3 inhibitors is currently under clinical investigations in relapsed/refractory AML (NCT03735875; NCT03625505).

Olverembatinib (HQP1351) is a novel, orally bioavailable, third-generation breakpoint cluster region protein-Abelson-murine leukemia 1 (BCR-ABL1) tyrosine kinase inhibitor (TKI). It is currently under investigation in multiple clinical trials for chronic myeloid leukemia (CML; NCT04260022; NCT03883087; NCT04126681; NCT03883100). As a multikinase inhibitor, HQP1351 has also demonstrated potent inhibition on FLT3, fibroblast growth factor receptor, KIT and several other oncogenic kinases [29–31]. Lisaftoclax (APG-2575), a novel selective BCL-2 inhibitor developed by Ascentage Pharma [32], is currently being tested clinically for several hematologic malignancies, including relapsed/refractory AML (NCT04215809, NCT04494503, NCT04501120). In a phase 1 clinical trial (NCT03537482), APG-2575 has demonstrated clinical activity and showed a favorable safety profile in patients with hematologic malignancies. APG-2575 was well tolerated up to 1200 mg/day, and no tumor lysis syndrome (TLS) was observed, even with a quick, daily ramp-up dosing schedule [33].

In the present study, we explored the anti-leukemic activity of FLT3 inhibition by HQP1351 alone or in combination with BCL-2 inhibitor APG-2575, in preclinical models of *FLT3-ITD* mutant AML. Our data demonstrates the synergistic anti-leukemic effects of HQP1351 and APG-2575 in *FLT3-ITD* mutant AML and provides scientific rationale to support further clinical investigations of the combination therapy in patients with *FLT3-ITD* mutant AML.

Materials and methods

Cell lines and reagents

Human AML cell lines were purchased from the American Type Culture Collection (ATCC). MV-4–11 cells were propagated in Iscove's Modified Dulbecco's Medium supplemented with 10% fetal calf serum (FCS). Other cell lines were propagated in Roswell Park Memorial Institute (RPMI) 1640 medium containing 10% FCS. All experiments utilized genetically authenticated, microbial-free cells in their exponential phases of growth. APG-2575 and HQP1351 (Ascentage Pharma, Jiangsu, China) were dissolved in dimethyl sulfoxide (DMSO) for *in vitro* experiments or suspended in 0.2% hydroxypropyl methylcellulose (HPMC) for *in vivo* studies.

Cellular apoptosis analysis

In 24-well plates, MV-4–11 or MOLM-13 cells were seeded at a density of 100,000 cells in 500 μl of medium per well. Cells were allowed to establish overnight and treated with 10 nM APG-2575 or 3 nM HQP1351, alone or in combination, for 24 h. Cells were then stained with Annexin V-fluorescein isothiocyanate (FITC)/propidium iodide (PI) Apoptosis Detection Kit, and apoptotic cells were analyzed by flow cytometry. Briefly, cells were washed once with cold phosphate-buffered saline (PBS) and incubated for 15 min at room temperature with Annexin V-FITC/PI in binding buffer. Cells were then analyzed on an Attune NxT Flow Cytometer (Thermo Fisher) using FlowJo™ software analysis software (FlowJo, LLC; Ashland, OR). Results were expressed as percentages of Annexin V^+/PI^+ cells. Experiments were performed in duplicate in three independent experiments.

Western blotting analysis

The assay was performed as described previously [34]. Cells were collected and lysed in radioimmunoprecipitation assay (RIPA) lysis buffer containing 1% protease inhibitor cocktail, 1% InStab™ phosphatase inhibitor cocktail, and 1% phenyl-methyl-sulfonyl fluoride (PMSF). Protein concentration was quantitated using a bicinchoninic acid (BCA) protein assay kit (Beyotime, Cat# P0010). Equal amounts of soluble protein were loaded and separated using 4–20% sodium dodecyl sulphate polyacrylamide gel electrophoresis (SDS-PAGE), followed by transfer to a polyvinylidene difluoride (PVDF) membrane. Blots were then incubated with primary antibodies against FLT3, phosphorylated FLT3 (P-FLT3), STAT5, phosphorylated STAT5 (P-STAT5), AKT, phosphorylated AKT (P-AKT), extracellular signal-regulated kinase (ERK1/2), phosphorylated ERK1/2 (P-ERK1/2), poly (ADP-ribose) polymerase (PARP), Caspase-3, myeloid-cell leukemia 1 (MCL-1), and β-Actin. Anti-rabbit or anti-mouse horseradish peroxidase (HRP)–conjugated secondary antibodies (Yeasen, Cat# 33101ES60 and 33201ES60) were used at a 1:5000 dilution. Immunoreactive proteins were visualized using an Azure c300 Chemiluminescent Western Blot Imaging System (Azure Biosystems Inc, Dublin, CA).

AML cell line-derived xenograft (CDX) models

All animal experiments were conducted at the animal facility of GenePharma (Suzhou, China). Protocols and experimental procedures involving the care and use of animals were approved by the GenePharma Institutional Animal Care and Use Committee. Animals were allowed to acclimate to the environment for at least 3 days then transferred to a temperature-(20–26 °C) and humidity (40–60%, relative humidity)-controlled specific-pathogen-free (SPF) room with a 12 h light/12 h dark cycle during the experimental period. Mice were housed in cages, with no more than five per cage and had free access to sterile drinking water and food.

For the subcutaneous model, MV-4–11 cells (1×10^6) were injected

subcutaneously into the right flanks of 6–8-week old female nonobese diabetic/severe combined immunodeficient (NOD/SCID mice). Mice were randomly grouped when tumor volume reached a mean of 100–150 mm^3. For monotherapy, tumor-bearing mice were treated with 10 or 30 mg/kg HQP1351 orally, QOD for 22 consecutive days. For the combination treatment, mice were treated with 10 mg/kg HQP1351 QOD and 100 mg/kg APG-2575 QD alone or in combination for 19 consecutive days. Tumor volumes were measured by caliper twice a week and calculated using the formula:

$$\text{Tumor Volume}\left(mm^3\right) = \left(a \times b^2\right) / 2$$

where a is the long diameter of the tumor and b is the short diameter. Mice were humanely euthanized when their body weight loss exceeded 20% or a subcutaneous tumor volume reached 2000 mm^3.

As a measurement of anti-tumor efficacy, the T/C ratio (treatment/control) value was calculated as follows:

$$\frac{T}{C}\% = \frac{RTV\ treated\ tumors}{RTV\ control\ tumors} \times 100$$

Where RTV is the mean relative tumor volume which is in turn expressed as the ratio of Vt/V1, where Vt is the average tumor volume at a certain time point (Day t) and V1 is the average tumor volume on the first day of treatment (Day 1). Tumor growth inhibition (TGI) was calculated as:

$$TGI\ \% = (1 - T / C) \times 100$$

For the MOLM-13 systemic AML model, 6- to 8-week old female NOD/SCID mice were pretreated with cyclophosphamide (150 mg/kg, intraperitoneally) for 2 consecutive days, and intravenously inoculated with 1×10^7 of MOLM-13 cells. After 3 days, tumor-bearing mice were randomized and receive indicated treatments. For monotherapy, mice were treated with vehicle, 3, 10, or 30 mg/kg HQP1351 orally QOD for 21 consecutive days. For combination, mice were treated with vehicle, 10 mg/kg HQP1351, or 100 mg/kg APG-2575 alone or in combination by oral administration for 21 consecutive days and monitored daily for development of hind-limb paralysis or abdominal swelling resulting from disease progression, as well as body weight loss greater than 20%. These clinical manifestations served as humane endpoints.

AML patient-derived xenograft (PDX) model

The AML PDX model (AM7577, *FLT3-ITD*, $TP53^{WT}$, $IDH2^{R140Q}$, $DNMT3A^{R882H}$, $NPM1^{ins}$, $CEBPA^{ins}$) was performed at Crown Bioscience Inc. (Suzhou, China). Two million (2×10^6) AM7577 AML cells suspended in 0.1 ml sterile PBS were injected into 6- to 8-week-old female NOD/SCID mice through the tail vein. After 28 days, when the average proportion of human $CD45^+$ and $CD33^+$ cells in the peripheral blood reached approximately 0.5%, the tumor-bearing mice were randomized to 4 groups and treated with vehicle, 10 mg/kg HQP1351, 100 mg/kg APG-2575, or the combination for 28 consecutive days. Proportions of human $CD45^+$ and $CD33^+$ cells in the peripheral blood of each mouse were monitored by flow cytometry weekly. At the end of treatment, cells from spleen and bone marrow of two femurs were collected and lysed in 2 mL 1 × red-blood-cell lysis buffer at room temperature for 2 min, followed by centrifugation at 1000 rpm for 5 min. Supernatants were discarded and cell pellets were washed twice with cold PBS, followed by incubation with live/dead antibody for 15 min. Cells were then washed twice with PBS and incubated with FITC conjugated human CD45 and APC-conjugated human CD33 antibodies diluted in staining buffer (PBS containing 10% FBS and 2% EDTA) at 1:5 for 30 min on ice. After incubation, cells were washed twice with PBS and subjected to flow cytometry analysis on the Attune NxT Flow Cytometer. Data were analyzed using FlowJo software and reported as percentages of human $CD45^+$/$CD33^+$cells of total live cells.

Supplementary Table 1 provides further details regarding sources of materials.

Statistical analysis

Unpaired Student's *t* test was used to compare differences between treatment and control groups. One-way analysis of variance (ANOVA) followed by Games–Howell's posttest was used to assess the statistical significance between multiple treatment groups in MV-4–11 subcutaneous models. Survival curves of different treatment groups were compared using the log-rank test with Bonferroni's test for multiple comparisons. Data were analyzed using GraphPad Prism version 8.0 (GraphPad Software, San Diego, CA) or SPSS version 18.0 (IBM PASW Statistics for Windows; Chicago, IL USA). * $p<0.05$, ** $p<0.01$, *** $p<0.001$.

Results

HQP1351 induces apoptosis in FLT3-ITD mutant AML cells by inhibiting FLT3 signaling

HQP1351 was shown to selectively inhibit the proliferation of *FLT3-ITD* mutant leukemia cells over FLT3 wild-type cells in a previous study [31]. To investigate apoptosis induction by HQP1351 in *FLT3-ITD* mutant AML cells, MOLM-13 and MV-4–11 cells were treated with various concentrations of HQP1351 and cellular apoptosis was determined by Annexin V/PI staining. Treatment with HQP1351 from 1 to 100 nM dose-dependently increased the proportion of apoptotic cells in both MOLM-13 and MV-4–11 cells (Fig. 1A and B).

FLT3-ITD mutation causes constitutive activation of FLT3 and its downstream signaling proteins, thus, we investigated the inhibition of HQP1351 on FLT3 signaling pathways in MOLM-13 and MV-4–11 cells. As shown in Fig. 1C and D, HQP1351 dose-dependently inhibited the phosphorylation of FLT3 and its downstream signaling proteins ERK1/2, AKT, and STAT5 in both cell lines. Taken together, these data suggest that HQP1351 potently induces apoptosis and inhibits FLT3 kinase and its downstream signaling in *FLT3-ITD* mutant AML cells.

HQP1351 exhibits potent anti-leukemic activity in FLT3-ITD mutant AML cell line-derived xenograft models

We next investigated the *in vivo* anti-leukemic activity of HQP1351 against *FLT3-ITD* mutant AML in MV-4–11 subcutaneous xenograft and MOLM-13 systemic model in NOD/SCID mice. In the MV-4–11 subcutaneous model, treatment with HQP1351 effectively suppressed the growth of tumor volume with a T/C of 28.6% at 10 mg/kg dose at the conclusion of the study (Day 22). HQP1351 further decreased tumor volume at 30 mg/kg dose, with a T/C of 0.4% ($p < 0.05$ vs. vehicle control) on Day 22 (Fig. 2A). Tumor weights were also significantly decreased by the treatment with HQP1351 at both doses at study termination (Fig. 2B). Mean tumor weights were reduced to 0.67 g and to an undetectable level by 10 mg/kg and 30 mg/kg HQP1351, respectively. No significant changes in body weight were observed in any treatment groups (Supplementary Fig. 1).

Anti-leukemic activity of HQP1351 against *FLT3-ITD* mutant AML was further evaluated in MOLM-13 systemic model, tumor burden was assessed by analyzing the proportion of human CD45+ cells in the spleen and bone marrow of mice injected with MOLM-13 cells. Compared to vehicle control, HQP1351 dose dependently decreased tumor burden in spleen and bone marrow and improved the survival of tumor bearing mice. At doses of 3 mg/kg, 10 mg/kg, and 30 mg/kg, HQP1351 decreased tumor burden (% of $hCD45^+$ cells) in the bone marrow from 7.17% (vehicle control) to 3.09%, 0.11%, and 0.08%, respectively (Fig. 2C). A similar decrease was observed in the spleen, with the percentage of human $CD45^+$ cells decreasing from 1.12% (vehicle control), to 0.65%, 0.11%, and 0.10%, respectively. (Fig. 2D). Compared to vehicle control, HQP1351 at 3 mg/kg, 10 mg/kg, and 30

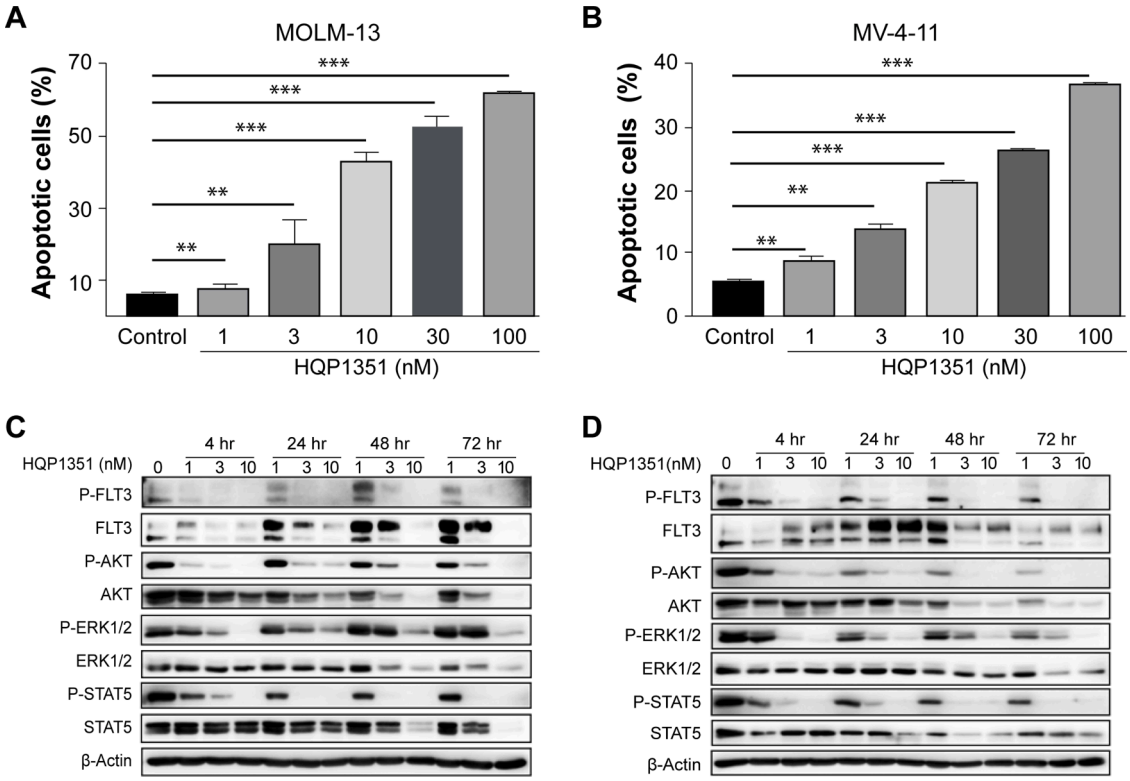

Fig. 1. HQP1351 induces apoptosis in *FLT3-ITD* mutant AML cells by inhibiting FLT3 signaling. **A and B.** MOLM-13 **(A)** and MV-4–11 **(B)** cells were exposed to increasing concentrations of HQP1351 for 24 h, cells were harvested and subjected to Annexin V/PI staining, the percentage of apoptotic cells was analyzed by flow cytometry. **C and D.** Phosphorylation of FLT3 and its downstream signaling proteins ERK1/2, AKT and STAT5 were analyzed by western blotting in MOLM-13 **(C)** and MV-4–11 **(D)** Cells exposed to HQP1351 at indicated concentrations and time points, β-Actin was used as an internal control. * $p < 0.05$, ** $p < 0.01$, *** $p < 0.001$.

mg/kg dose-dependently increased the median survival time of tumor-bearing mice by 2 days ($p = 0.0069$),7.5 days ($p < 0.0001$), and 16.5 days ($p < 0.0001$), respectively (Fig. 2E). Taken together, these data suggest that HQP1351 was well tolerated and exhibited potent anti-leukemic activity in *FLT3-ITD* mutant AML models *in vivo*.

HQP1351 and APG-2575 synergistically induce apoptosis in FLT3-ITD mutant AML cells

The foregoing results suggest that HQP1351 is a potent FLT3 inhibitor with anti-leukemic activity *in vitro* and *in vivo*. However, clinical experiences with FLT3 inhibitors monotherapy has shown a short duration of response and a high rate of relapse [17,20], suggesting that combination strategies may be needed to improve clinical outcomes. Previous studies have suggested a synergistic effect of BCL-2 inhibition and FLT3 inhibition in preclinical models of *FLT3-ITD* mutant AML [24]. Therefore, we next sought to investigate the combination of HQP1351 and BCL-2 inhibitor APG-2575 in *FLT3-ITD* mutant AML models.

We first evaluated induction of apoptosis by the combination of HQP1351 and APG-2575 in *FLT3-ITD* mutant AML cells. As shown in Fig. 3, either single agent of HQP1351 or APG-2575 induced apoptosis in MOLM-13 and MV-4–11 cells, while the percentage of apoptotic cells was greatly increased by the combination. A similar combination effect was observed with FLT3 selective inhibitor quizartinib and APG-2575 in MOLM-13 cells. Quizartinib or APG-2575 alone induced cellular apoptosis, and quizartinib further enhanced APG-2575-induced apoptosis when combined with APG-2575 (Supplementary Fig. 2A). In contrast, the same concentration of FGFR inhibitors erdafitinib or infigratinib alone had no significant effect on MOLM-13 cells, and neither FGFR inhibitor further increased cellular apoptosis when combined with APG-2575 (Supplementary Fig. 2B and C). Taken together, these results demonstrate that HQP1351, as a FLT3 inhibitor, synergizes with APG-2575 to augment apoptosis in *FLT3-ITD* mutant AML cells.

Synergistic anti-leukemic effect of APG-2575 and HQP1351 in FLT3-ITD mutant AML models in vivo

We further evaluated the *in vivo* anti-leukemic activity of HQP1351 combined with APG-2575 in AML cell line-derived xenograft models. In the MV-4–11 subcutaneous xenograft model, HQP1351 or APG-2575 alone suppressed tumor growth with a T/C of 22.0% and 59.0% respectively, whereas the combination nearly completely eradicated the tumors with a T/C of 2.8% (Fig. 4A). Consistent with tumor volume inhibition, tumor weights were reduced at study conclusion, HQP1351 plus APG-2575 showed greater inhibition compared to each agent alone (Fig. 4B). Similar anti-leukemic activity was observed in MOLM-13 systemic model, in which either HQP1351 or APG-2575 alone extended the survival of tumor-bearing mice, and the combination further prolonged survival (Fig. 4C and Supplementary Table 3). Treatment with either HQP1351, APG-2575, or combination of both agents was well tolerated in both AML models with no obvious pharmacokinetic interaction observed between HQP1351 and APG-2575 in the MV-4–11 xenograft model (Supplementary Fig. 3 and Supplementary Table 2). Collectively, these data suggest the synergistic anti-leukemic effect of APG-2575 and HQP1351 *in vivo* in *FLT3-ITD* mutant AML models without additional toxicity based on no changes in mouse body weight.

Synergistic anti-leukemic effect of HQP1351 and APG-2575 in FLT3-ITD mutant AML patient derived xenograft (PDX) model

Potential synergy between APG-2575 and HQP1351 was further

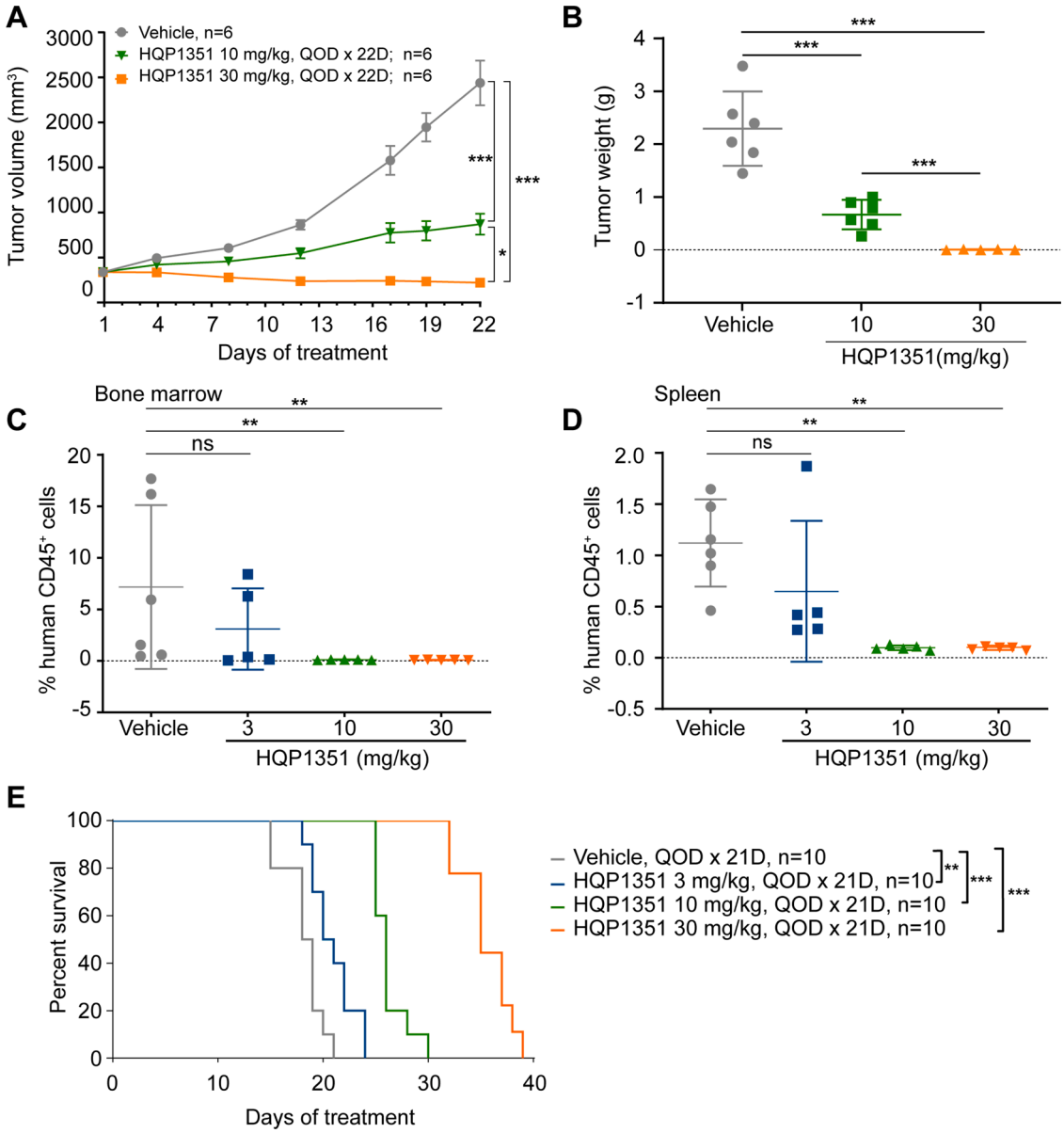

Fig. 2. HQP1351 exhibits potent anti-leukemic activity *in vivo* in *FLT3-ITD* mutant AML xenograft models. **A.** Tumor growth curve of MV-4–11 subcutaneous xenograft tumors in NOD/SCID mice treated with vehicle control or the indicated doses of HQP1351; tumor volume was monitored at indicated time points. **B.** Same as (A), but the tumor weight was assessed at the end of the experiment. **C and D.** Flow cytometric quantification of the percentage of human CD45$^+$ cells in bone marrow **(C)** and spleen **(D)** of NOD/SCID mice injected with MOLM-13 cells via tail vein and treated with vehicle control or the indicated doses of HQP1351 for 21 days. **E.** NOD/SCID mice injected with MOLM-13 cells via the tail vein were treated with vehicle control or the indicated doses of HQP1351 for 21 days and then the treatments were stopped. The survival time of tumor-bearing mice were subsequently monitored until the animals met a humane endpoint. QOD, every other day, * $p < 0.05$, ** $p < 0.01$, *** $p < 0.001$.

evaluated in *FLT3-ITD* mutant AML PDX model AM7577 (*FLT3-ITD, TP53^{WT}, IDH2^{R140Q}, DNMT3^{AR882H}, NPM1^{ins}, CEBPA^{ins}*), which can more accurately replicate tumor progression and tumor cell diversity. Compared to vehicle control, all treatments decreased tumor burden (proportion of human CD45$^+$/CD33$^+$ cells) in peripheral blood through the end of study (Day 29). Mean percentages of human CD45$^+$/CD33$^+$ cells at Day 29 were 50.42% (vehicle control), and 22.56%, 3.77%, and 0.08% for APG-2575, HQP1351, and the combination, respectively (Fig. 5A). At the termination of the study, spleen weights were significantly reduced in all treatment groups ($p < 0.01$) compared to vehicle control (Fig. 5B). Combination treatment further reduced spleen weight compared to HQP1351 or APG-2575 monotherapy. Tumor burden in peripheral blood, spleen and bone marrow were analyzed by flow cytometry at study conclusion or upon reaching the endpoint. As shown in Fig. 5C and 5D, HQP1351 alone significantly reduced tumor burdens in peripheral blood, spleen, and bone marrow (each $p < 0.01$ vs vehicle control), and HQP1351 combined with APG-2575 significantly further decreased tumor burden ($p < 0.05$-vs either monotherapy).

Taken together, these results suggest synergistic effects between HQP1351 and APG-2575 in an AML PDX model with *FLT3-ITD* mutation. Notably, the combination of APG-2575 and HQP1351 significantly reduced tumor burden in bone marrow cells, indicating that the combination owns the capability to eradicate minimal residual disease (MRD) in AML, which may lead to a more durable response clinically.

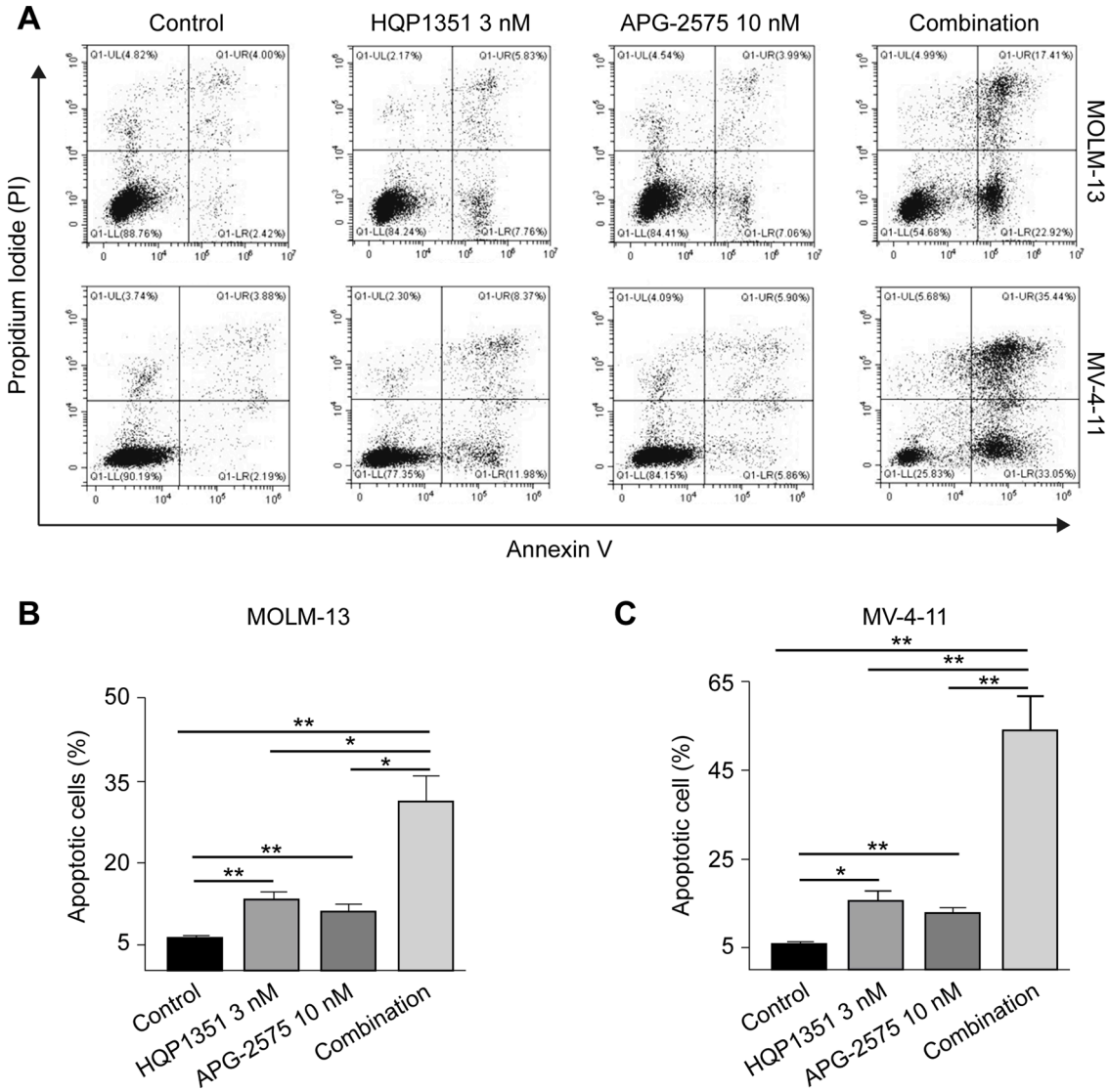

Fig. 3. HQP1351 and APG-2575 synergistically induce apoptosis in *FLT3-ITD* mutant AML cells. **A.** Representative flow cytometry results of cellular apoptosis in MOLM-13 cells and MV-4–11 cells. Cells were treated with HQP1351, APG-2575 or the combination for 24 h, and then subjected to Annexin V and PI staining. **B and C.** Same as (A), but the quantification of the percentage of apoptotic cells in MOLM-13 **(B)** and MV-4–11 **(C)** cells are shown. * $p < 0.05$, ** $p < 0.01$, *** $p < 0.001$.

HQP1351 downregulates MCL-1 expression and enhances APG-2575 induced apoptosis in FLT3-ITD mutant AML cells

Upregulation of anti-apoptotic protein MCL-1, as well as BCL extra-large (BCL-xL) is considered a pivotal mechanism of resistance to BCL-2 inhibition [35]. Therefore, to investigate the molecular mechanisms underlying the synergy effect of HQP1351 and APG-2575, we examined phosphorylation of FLT3 and its downstream signaling proteins ERK1/2, AKT and STAT5, anti-apoptotic proteins BCL-2, BCL-xL and MCL-1, and hallmarks of apoptosis in *FLT3-ITD* mutant AML cells.

Single agent HQP1351 inhibited phosphorylation of FLT3 and its downstream signaling, as indicated by the decreased phosphorylation of ERK1/2, AKT and STAT5 in MV-4–11 and MOLM-13 cells (Fig. 6). In both cell lines, BCL-2 inhibition by APG-2575 slightly increased apoptosis, and markedly augmented the expression of MCL-1, thereby preventing apoptosis. In combination treatment, HQP1351 further downregulated the expression of MCL-1 and BCL-xL induced by APG-2575 treatment, resulting in enhanced apoptosis, as evidenced by increased cleavage of caspase 3 and PARP, hallmarks of cellular apoptosis (Fig. 6). Taken together, these data suggest that HQP1351 synergizes with APG-2575 to potentiate cellular apoptosis in *FLT3-ITD* mutant AML cells by downregulating anti-apoptotic proteins MCL-1 and BCL-xL.

Discussion

The present study investigated the anti-leukemic activity of HQP1351 and its combination with BCL-2 inhibitor APG-2575 *in vitro* using *FLT3-ITD* mutant AML cell lines and *in vivo* using cell line- and patient-derived xenograft models. Our data strongly suggest that HQP1351 exhibits potent anti-leukemic activity against *FLT3-ITD* mutant AML by inhibiting FLT3 kinase activity, and that HQP1351 synergizes with BCL-2 inhibitor APG-2575 to potentiate cellular apoptosis in *FLT3-ITD* mutant AML models by downregulating MCL-1 and BCL-xL.

In our present study, single-agent of HQP1351 has demonstrated potent anti-leukemic activity in preclinical models of *FLT3-ITD* mutant AML. HQP1351 inhibited phosphorylation of FLT3 and downstream signaling pathways, resulting in suppression of cellular proliferation and induction of apoptosis, suggesting that the anti-leukemic activity of HQP1351 is through on-target inhibition on FLT3 signaling. Moreover, research from Dr. Ding's laboratory has shown that HQP1351 can also

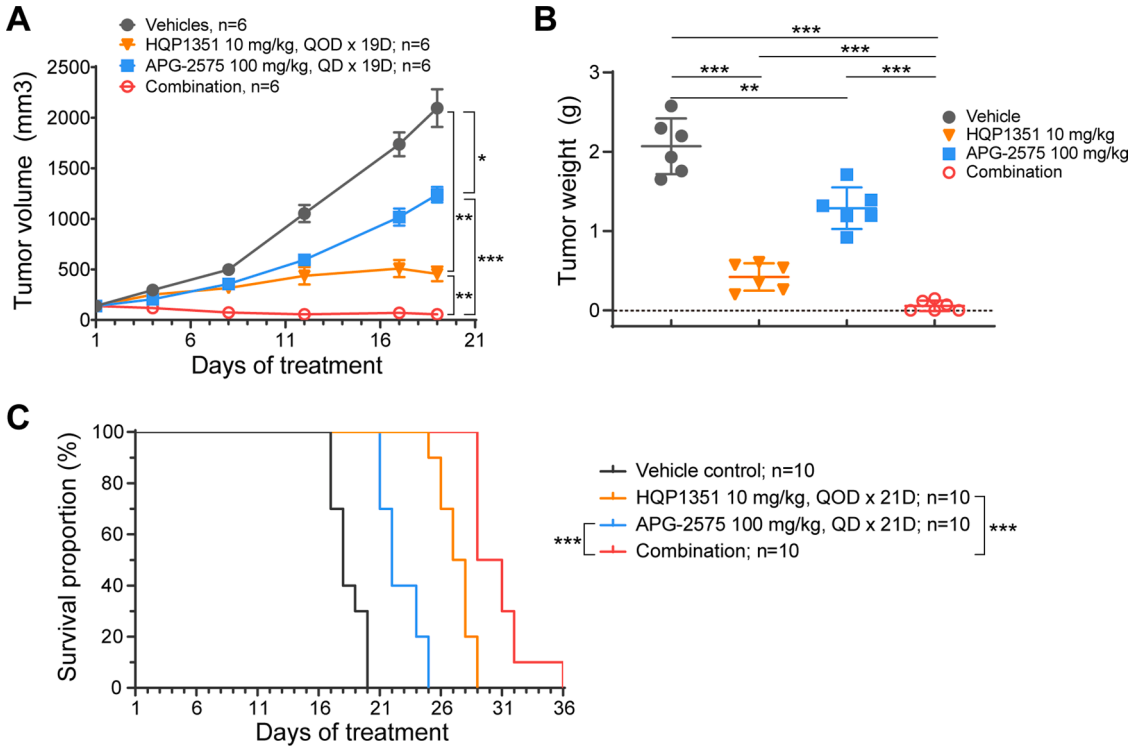

Fig. 4. Synergistic anti-leukemic effect of HQP1351 and APG-2575 in *FLT3-ITD* AML models. **A.** Tumor growth curves of MV-4–11 subcutaeous xenograft tumors in NOD/SCID mice treated with vehicle control, HQP1351, APG-2575, or the combination for 19 consecutive days, and tumor volume was monitored every 4 days. **B.** Same as (A), but the tumor weight was assessed at the end of the experiment. **C.** Survival of NOD/SCID mice injected with MOLM-13 cells via the tail vein and treated with HQP1351, APG-2575, or the combination for 21 consecutive days. QOD, every other day, $^{*}p < 0.05$, $^{**}p < 0.01$, $^{***}p < 0.001$.

overcome FLT3 inhibitors resistance conferred by *FLT3-TKD* point mutations, including *FLT3-D835N/H/R/G/A, F691I* and *G697R* [31]. These preclinical studies together suggest that HQP1351 is an effective FLT3 inhibitor targeting both FLT3 with ITD or TKD mutations. Since HQP1351 is now under clinical investigations for CML and gastrointestinal stromal tumor and exhibits good safety profile, our data suggest that HQP1351 may be used as an alternative FLT3 inhibitor in clinic for AML patients with *FLT3* mutations.

Venetoclax plus azacitidine (AZA) has become a major first-line therapeutic option for elderly patients with AML. However, the 3-year survival rate remains < 40% due to acquired resistance [26,36,37]. Studies investigating the underlying mechanisms have revealed that mutations in *FLT3-ITD* is a major cause of the acquired resistance to venetoclax in patients with AML [38]. Patients with AML who have baseline *FLT3-ITD* mutations showed no measurable reduction in bone marrow blasts after venetoclax treatment [39]. In addition, new *FLT3-ITD* mutations emerged in relapsed patients following venetoclax monotherapy or combined therapy with LDAC [40,41], suggesting *FLT3-ITD* mutations are associated with both primary and acquired resistance to venetoclax. In preclinical settings, FLT3 inhibitors in combination with venetoclax have shown synergistic anti-leukemic effects in *FLT3-ITD* mutant cell lines or xenograft tumor models [24,27,28]. Moreover, clinical studies evaluating combination of FLT3 inhibitors and venetoclax have demonstrated safety and activity in patients with relapsed/refractory (R/R) *FLT3*-mutant (9 patients with *FLT3-ITD* mutation, 1 patient with *FLT3-TKD* mutation) AML with a composite CR rate of 85%, indicating FLT3 inhibition in combination with BCL-2 inhibitors is a promising strategy to improve outcomes and overcome resistance in patients with *FLT3-ITD* mutant AML [42,43].

In agreement with previous reports, our data suggest synergistic effects of BCL-2 inhibition (by APG-2575) when combined with FLT3 inhibition (by HQP1351) in preclinical models of *FLT3-ITD* mutant AML. HQP1351 inhibits the phosphorylation of FLT3 and enhanced APG-2575-induced cellular apoptosis in two *FLT3-ITD* mutant AML cell lines MOLM-13 and MV-4–11. In the MV-4–11 subcutaneous xenograft model, HQP1351 combined with APG-2575 significantly suppressed tumor growth, which was superior to tumor growth suppression induced by either HQP1351 or APG-2575 alone. In an AML PDX model with a *FLT3-ITD* mutation, limited anti-leukemic activity was observed in the APG-2575 treatment group, whereas HQP1351 as a single agent showed impressive anti-leukemic activity. After conventional treatment in patients with AML, relapse of MRD is a major challenge, and the bone marrow (BM) is consider to be a major site for MRD in clinic [44]. In an AML PDX model, HQP1351 monotherapy eliminated tumor cells from the peripheral blood and spleen (<5% $hCD45^{+}/hCD33^{+}$ cells) but not the bone marrow (BM). Notably, the combination of APG-2575 and HQP1351 completely eliminated leukemic cells from the bone marrow microenvironment (<1% $hCD45^{+}/hCD33^{+}$ cells). Although *FLT3* is the most mutated gene in AML and is associated with venetoclax resistance, the expansion of resistant clones in other subtype of AML with *IDH1/2, NF1*, or other gene mutations have also been associated with resistance to venetoclax [38]. Therefore, rational combination therapies will be needed to improve the outcome of venetoclax and other BCL-2 inhibitors in AML with distinct genetic alterations.

The underlying mechanism of resistance to BCL-2 inhibition is mainly determined by the upregulation of anti-apoptotic proteins MCL-1 and/or BCL-xL [35]. Venetoclax liberates BIM from BCL-2, but the freed BIM may be sequestered by MCL-1 and/or BCL-xL to prevent apoptosis. Therefore, simultaneous inhibition of BCL-2 with MCL-1 and/or BCL-xL is required for effective induction of apoptosis [45].

FLT3 activation is known to promote cellular proliferation and survival by activating oncogenic signaling pathways, including MAPK and PI3K. Unlike *FLT3-TKD* mutations and ligand stimulated FLT3 activation, *FLT3-ITD* mutations also specifically activate STAT5 and promote the expression of MCL-1 in AML cells [46]. FLT3 inhibitors in combination with venetoclax synergistically increased apoptosis by inhibiting

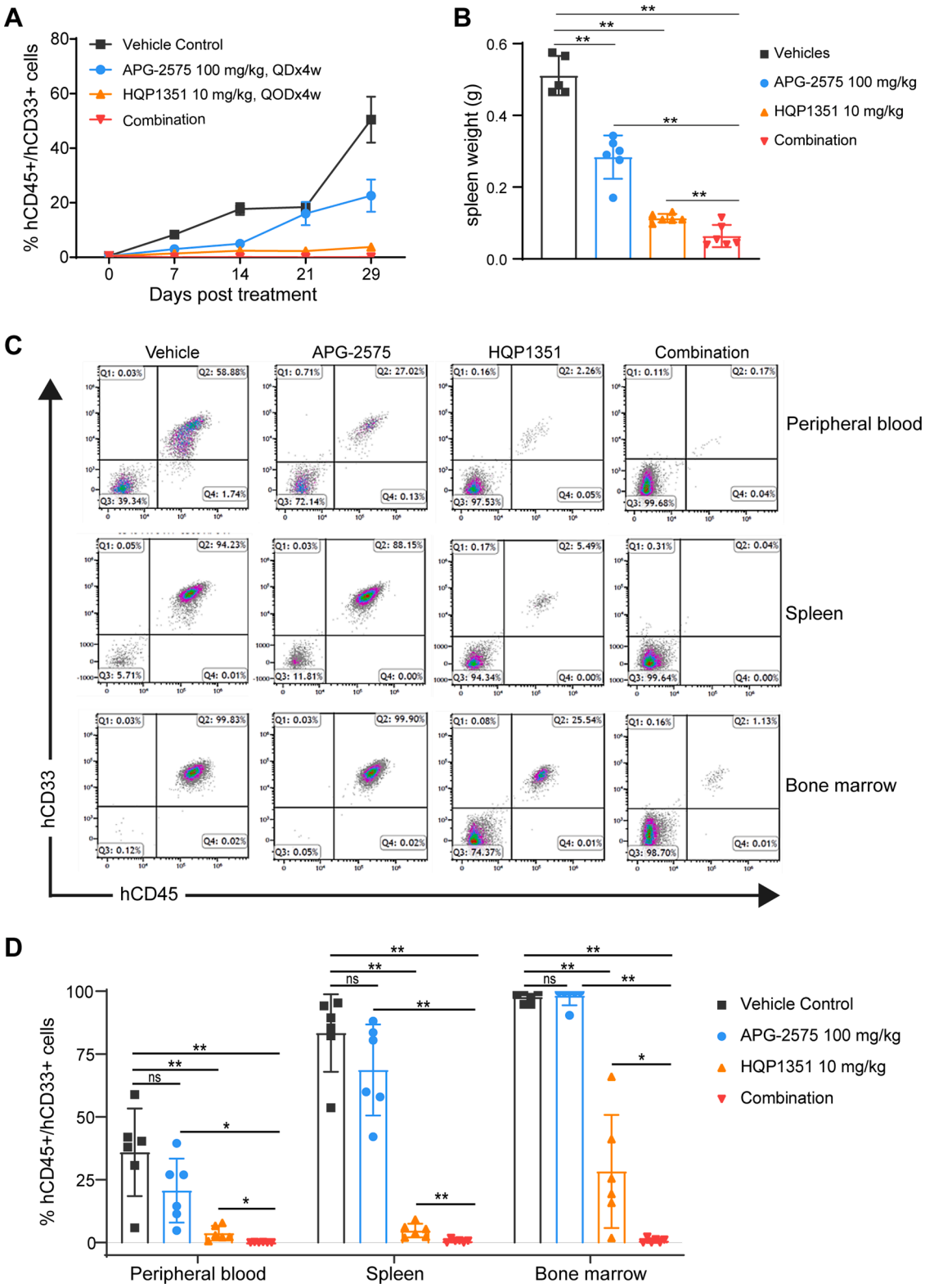

Fig. 5. Synergistic anti-leukemic effect of HQP1351 and APG-2575 in *FLT3-ITD* mutant AML PDX model. **A.** The proportion of human CD45$^+$ and CD33$^+$ cells in peripheral blood of NOD/SCID mice injected with patient-derived AML cells (AM7577) via the tail vein. After tumor cells were established, mice were randomized to four groups and treated with 10 mg/kg HQP1351, 100 mg/kg APG-2575, or the combination for 28 consecutive days. The proportion of human CD45$^+$ and CD33$^+$ cells in peripheral blood of each mouse was monitored by flow cytometry weekly. **B.** Same as **(A)**, but the spleen weight was measured at the termination of the experiment. Three mice from the vehicle group and one mouse from the APG-2575-treated group were euthanized before the end of the experiment as they reached the endpoint. **C.** Same as **(A)**, the proportions of human CD45$^+$ and CD33$^+$ cells in peripheral blood, spleen and bone marrow were analyzed by FACS at the termination or upon reaching the endpoint. Representative images are shown. **D.** Quantitation of the percentage of human CD45$^+$ and CD33$^+$ cells in peripheral blood, spleen and bone marrow. QD, daily, QOD, every other day. Each group was compared to vehicle control by unpaired Student's *t*-test. ns, not significant; $^*p < 0.05$, $^{**}p < 0.01$, $^{***}p < 0.001$.

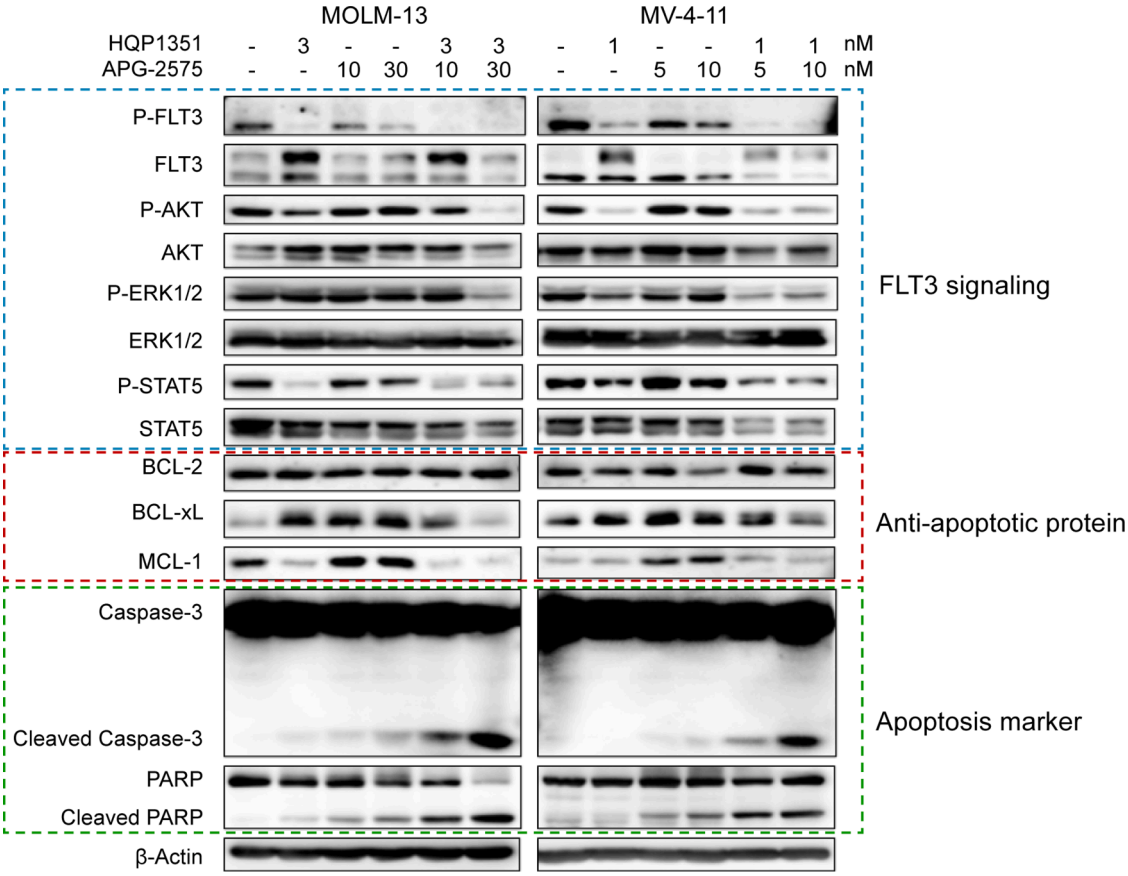

Fig. 6. HQP1351 enhances APG-2575-induced apoptosis in *FLT3-ITD* mutant AML cells by downregulating MCL-1 and BCL-xL. MOLM-13 and MV-4–11 cells were exposed to HQP1351, APG-2575 or the combination at various concentrations for 24 h. Phosphorylation of FLT3 and its downstream signaling proteins ERK1/2, AKT, and STAT5; anti-apoptotic proteins BCL-2, BCL-xL, and MCL-1; and hallmarks of apoptosis (cleaved caspase-3 and PARP) were analyzed by western blotting. β-Actin was used as an internal control.

MCL-1 in AML [27,28]. Similarly, our study also shows that HQP1351 inhibited FLT3, which in turn suppressed the activation of STAT5 and downregulated the expression of MCL-1, thus synergizing with BCL-2 inhibitor APG-2575 to potentiate apoptosis in *FLT3-ITD* mutant AML cells.

Conclusion

The present study suggests that FLT3 inhibition by HQP1351 downregulates MCL-1 and otherwise synergizes with BCL-2 inhibitor APG-2575 to potentiate cellular apoptosis in *FLT3-ITD* mutant AML. These results provide a scientific foundation for further clinical investigation of the combination of HQP1351 with APG-2575 in patients with *FLT3-ITD* mutant AML.

CRediT authorship contribution statement

Douglas D. Fang: Conceptualization, Methodology, Investigation, Formal analysis, Validation, Data curation, Supervision, Project administration, Writing – original draft. **Hengrui Zhu:** Conceptualization, Methodology, Investigation, Formal analysis, Validation, Data curation, Supervision, Project administration, Writing – original draft. **Qiuqiong Tang:** Methodology, Validation, Writing – review & editing. **Guangfeng Wang:** Methodology, Validation, Writing – review & editing. **Ping Min:** Methodology, Investigation, Writing – review & editing. **Qixin Wang:** Methodology, Investigation, Writing – review & editing. **Na Li:** Methodology, Investigation, Writing – review & editing. **Dajun Yang:** Supervision, Visualization, Writing – review & editing, Funding acquisition. **Yifan Zhai:** Supervision, Visualization, Writing – review & editing, Funding acquisition.

Declaration of Competing Interest

The authors are full-time employees and stockholders of Ascentage Pharma.

Acknowledgments

We thank Kaikai Xu for performing cellular apoptosis assays for the manuscript revisions. We thank Ascentage CMC and Analytic Center colleagues for synthesizing HQP1351, APG-2575 and providing the quality control. Ashutosh K. Pathak, MD, PhD, MBA, FRCP (Edin.), Stephen W. Gutkin, and Ndiya Ogba, PhD, with Ascentage provided further substantive input in manuscript research and preparation. Preparation of this study report was informed by Animal Research: Reporting In Vivo Experiments (ARRIVE) guidelines for preclinical research.

Funding

The research was funded by Ascentage Pharma (Suzhou) Co., Ltd, where all authors were employees at the time the study was conducted.

Supplementary materials

Supplementary material associated with this article can be found, in the online version, at doi:10.1016/j.tranon.2021.101244.

References

[1] I. De Kouchkovsky, M. Abdul-Hay, Acute myeloid leukemia: a comprehensive review and 2016 update', Blood Cancer J. 6 (7) (2016) e441.
[2] R.L. Siegel, K.D. Miller, A. Jemal, Cancer statistics, 2020, CA Cancer J. Clin. 70 (1) (2020) 7–30.
[3] R. Kihara, et al., Comprehensive analysis of genetic alterations and their prognostic impacts in adult acute myeloid leukemia patients, Leukemia 28 (8) (2014) 1586–1595.
[4] M. Levis, D. Small, FLT3: ITDoes matter in leukemia, Leukemia 17 (9) (2003) 1738–1752.
[5] Y. Yamamoto, et al., Activating mutation of D835 within the activation loop of FLT3 in human hematologic malignancies, Blood 97 (8) (2001) 2434–2439.
[6] C. Choudhary, et al., Signal transduction of oncogenic Flt3, Int. J. Hematol. 82 (2) (2005) 93–99.
[7] F. Hayakawa, et al., Tandem-duplicated Flt3 constitutively activates STAT5 and MAP kinase and introduces autonomous cell growth in IL-3-dependent cell lines, Oncogene 19 (5) (2000) 624–631.
[8] M. Mizuki, et al., Flt3 mutations from patients with acute myeloid leukemia induce transformation of 32D cells mediated by the Ras and STAT5 pathways, Blood 96 (12) (2000) 3907–3914.
[9] S.P. Whitman, et al., Absence of the wild-type allele predicts poor prognosis in adult de novo acute myeloid leukemia with normal cytogenetics and the internal tandem duplication of FLT3: a cancer and leukemia group B study, Cancer Res. 61 (19) (2001) 7233–7239.
[10] S. Kayser, et al., Insertion of FLT3 internal tandem duplication in the tyrosine kinase domain-1 is associated with resistance to chemotherapy and inferior outcome, Blood 114 (12) (2009) 2386–2392.
[11] J.P. Patel, et al., Prognostic relevance of integrated genetic profiling in acute myeloid leukemia, N. Engl. J. Med. 366 (12) (2012) 1079–1089.
[12] V. Rockova, et al., Risk stratification of intermediate-risk acute myeloid leukemia: integrative analysis of a multitude of gene mutation and gene expression markers, Blood 118 (4) (2011) 1069–1076.
[13] I. Rinaldi, et al., Prognostic significance of Fms-like tyrosine kinase 3 internal tandem duplication mutation in non-transplant adult patients with acute myeloblastic leukemia: a systematic review and meta-analysis, Asian Pac. J. Cancer Prev. 21 (10) (2020) 2827–2836.
[14] A. Elshoury, et al., Advancing treatment of acute myeloid leukemia: the future of FLT3 inhibitors, Expert Rev. Anticancer Ther. 19 (3) (2019) 273–286.
[15] M. Levis, Midostaurin approved for FLT3-mutated AML, Blood 129 (26) (2017) 3403–3406.
[16] A.I. Antar, et al., FLT3 inhibitors in acute myeloid leukemia: ten frequently asked questions, Leukemia 34 (3) (2020) 682–696.
[17] R.M. Stone, et al., Midostaurin plus chemotherapy for acute myeloid leukemia with a FLT3 mutation, N. Engl. J. Med. 377 (5) (2017) 454–464.
[18] A. Bazarbachi, et al., Clinical practice recommendation on hematopoietic stem cell transplantation for acute myeloid leukemia patients with FLT3-internal tandem duplication: a position statement from the acute leukemia working party of the European Society for Blood and Marrow Transplantation, Haematologica 105 (6) (2020) 1507–1516.
[19] V.E. Kennedy, C.C. Smith, FLT3 mutations in acute myeloid leukemia: key concepts and emerging controversies, Front. Oncol. 10 (2020), 612880.
[20] J. Zhao, Y. Song, D. Liu, Gilteritinib: a novel FLT3 inhibitor for acute myeloid leukemia, Biomark. Res. 7 (2019) 19.
[21] L. Campos, et al., High expression of bcl-2 protein in acute myeloid leukemia cells is associated with poor response to chemotherapy, Blood 81 (11) (1993) 3091–3096.
[22] A.W. Roberts, Therapeutic development and current uses of BCL-2 inhibition, Hematol. Am. Soc. Hematol. Educ. Program 2020 (1) (2020) 1–9.
[23] Y. Wei, et al., Targeting Bcl-2 proteins in acute myeloid leukemia, Front. Oncol. 10 (2020), 584974.
[24] L.T. Brinton, et al., Synergistic effect of BCL2 and FLT3 co-inhibition in acute myeloid leukemia, J. Hematol. Oncol. 13 (1) (2020) 139.
[25] A.H. Wei, et al., Venetoclax plus LDAC for newly diagnosed AML ineligible for intensive chemotherapy: a phase 3 randomized placebo-controlled trial, Blood 135 (24) (2020) 2137–2145.
[26] C.D. DiNardo, et al., Venetoclax combined with decitabine or azacitidine in treatment-naive, elderly patients with acute myeloid leukemia, Blood 133 (1) (2019) 7–17.
[27] J. Ma, et al., Inhibition of Bcl-2 synergistically enhances the antileukemic activity of Midostaurin and Gilteritinib in preclinical models of FLT3-mutated acute myeloid leukemia, Clin. Cancer Res. 25 (22) (2019) 6815–6826.
[28] R. Singh Mali, et al., Venetoclax combines synergistically with FLT3 inhibition to effectively target leukemic cells in FLT3-ITD+ acute myeloid leukemia models, Haematologica 106 (4) (2021) 1034–1046.
[29] X. Ren, et al., Identification of GZD824 as an orally bioavailable inhibitor that targets phosphorylated and nonphosphorylated breakpoint cluster region-Abelson (Bcr-Abl) kinase and overcomes clinically acquired mutation-induced resistance against imatinib, J. Med. Chem. 56 (3) (2013) 879–894.
[30] X. Liu, et al., Preclinical development of HQP1351, a multikinase inhibitor targeting a broad spectrum of mutant KIT kinases, for the treatment of imatinib-resistant gastrointestinal stromal tumors, Cell Biosci. 9 (2019) 88.
[31] Y. Wang, et al., GZD824 as a FLT3, FGFR1 and PDGFRalpha inhibitor against leukemia in vitro and in vivo, Transl. Oncol. 13 (4) (2020), 100766.
[32] Q. Luo, et al., A novel BCL-2 inhibitor APG-2575 exerts synthetic lethality with BTK or MDM2-p53 inhibitor in diffuse large B-cell lymphoma, Oncol. Res. 28 (4) (2020) 331–344.
[33] S. Ailawadhi, A.A.A. Chanan-Khan, Z. Chen, B. Huang, M. Konopleva, D. M. Brander, D. Rizzieri, M. Lasica, C.S.L. Tam, C.K. Yannakou, H. Miles Prince, M. S. Davids, Z. He, M. Lu, M. Ahmad, M. Li, Z. Liang, B. Mudenda, D. Yang, Y. Zhai, First-in-human study of lisaftoclax (APG-2575), a novel BCL-2 inhibitor (BCL-2i), in patients (pts) with relapsed/refractory (R/R) CLL and other hematologic malignancies (HMs), J. Clin. Oncol. 39 (15) (2021) 1.
[34] D.D. Fang, et al., MDM2 inhibitor APG-115 synergizes with PD-1 blockade through enhancing antitumor immunity in the tumor microenvironment, J. Immunother. Cancer 7 (1) (2019) 327.
[35] P. Bose, V. Gandhi, M. Konopleva, Pathways and mechanisms of venetoclax resistance, Leuk. Lymphoma 58 (9) (2017) 1–17.
[36] C.D. DiNardo, et al., Azacitidine and venetoclax in previously untreated acute myeloid leukemia, N. Engl. J. Med. 383 (7) (2020) 617–629.
[37] D.A. Pollyea, et al., Venetoclax with azacitidine or decitabine in patients with newly diagnosed acute myeloid leukemia: long term follow-up from a phase 1b study, Am. J. Hematol. 96 (2) (2021) 208–217.
[38] X. Zhang, et al., Not BCL2 mutation but dominant mutation conversation contributed to acquired venetoclax resistance in acute myeloid leukemia, Biomark. Res. 9 (1) (2021) 30.
[39] M. Konopleva, et al., Efficacy and biological correlates of response in a Phase II study of venetoclax monotherapy in patients with acute myelogenous leukemia, Cancer Discov. 6 (10) (2016) 1106–1117.
[40] B. Chyla, et al., Genetic biomarkers of sensitivity and resistance to venetoclax monotherapy in patients with relapsed acute myeloid leukemia, Am. J. Hematol. (2018).
[41] C.D. DiNardo, et al., Molecular patterns of response and treatment failure after frontline venetoclax combinations in older patients with AML, Blood 135 (11) (2020) 791–803.
[42] V.A. Guerra, C. DiNardo, M. Konopleva, Venetoclax-based therapies for acute myeloid leukemia, Best Pract. Res. Clin. Haematol. 32 (2) (2019) 145–153.
[43] A. Maiti, et al., Triplet therapy with venetoclax, FLT3 inhibitor and decitabine for FLT3-mutated acute myeloid leukemia, Blood Cancer J. 11 (2) (2021) 25.
[44] F. Ayala, et al., Contribution of bone microenvironment to leukemogenesis and leukemia progression, Leukemia 23 (12) (2009) 2233–2241.
[45] X. Niu, et al., Binding of released Bim to Mcl-1 is a mechanism of intrinsic resistance to ABT-199 which can be overcome by combination with daunorubicin or cytarabine in AML cells, Clin. Cancer Res. 22 (17) (2016) 4440–4451.
[46] G. Yoshimoto, et al., FLT3-ITD up-regulates MCL-1 to promote survival of stem cells in acute myeloid leukemia via FLT3-ITD-specific STAT5 activation, Blood 114 (24) (2009) 5034–5043.